ARTICLES

Characterization and Structure of Molecular Aggregates of a Tetracationic Porphyrin in LB Films with a Lipid Anchor

I. Prieto,[†] J. M. Pedrosa,[‡] M. T. Martín-Romero,[‡] D. Möbius,[§] and L. Camacho*[,‡]

Departamento de Química Física y Química Orgánica, Facultad de Ciencias, Campus Lagoas-Marcosende, Universidad de Vigo, E-36200 Vigo, Spain, Departamento de Química Física y Termodinámica Aplicada, Facultad de Ciencias, Universidad de Córdoba, Campus de Rabanales, Edificio C-3, E-14014 Córdoba, Spain, and Max-Planck-Institut für biophysikalische Chemie, Am Fassberg 11, D-37077 Göttingen, Germany

Received: June 21, 2000

In this paper, the formation of the different aggregates of a water-soluble tetracationic porphyrin, TMPyP, anchored to an anionic phospholipid matrix, DMPA, and assembled in LB films has been investigated. The use of different solid substrates such as hydrophilic glass and supports modified by the transfer of monolayers of several lipids has been employed to assemble the TMPyP molecules in the mixed monolayer with DMPA (in a molar ratio of 1:4) as monomer ($TMPyP^{4+}$), dimer, diprotonated monomer ($TMPyPH_2^{6+}$), and tetramer aggregates. The porphyrin is organized as a monomer ($TMPyP^{4+}$) when the mixed monolayer is directly transferred onto a hydrophilic glass plate. Also, if the glass and the porphyrin are separated by spacer layers such as a monolayer sequence EA↑/AA↓/EA↑/AA↓, the porphyrin monomer is identified. Porphyrin dimers are formed at the air−water interface in monolayers of 1:4 TMPyP/DMPA[20] and may be transferred to solid substrates by the transfer of this system on top of the DMPA monolayer, i.e., $(DMPA\downarrow/TD\uparrow)_n$. In these multilayers, a small fraction of porphyrin molecules is transferred as diprotonated monomer. Finally, the transfer on hydrophilic glass plates of 1:4 TMPyP/DMPA monolayers of the Y type assembled a packed tetramer of TMPyP. By applying the extended dipole approximation to the spectra measured, we proposed a model where the central planes of the two consecutive porphyrins are twisted by 22.5°, forming a helix.

Introduction

The study on the organic ultrathin films has recently attracted great interest due to the potential technological applications of these materials, e.g., in molecular photoelectronic devices, medical applications, and other appliances.[1−5] One of the main problems related with the fabrication of these organic films is controlling the orientation and aggregation of the molecules. This problem is particularly important in the case of porphyrins due to the high tendency of these molecules to form different types of aggregates. In recent years, the formation of aggregates of ionic porphyrins in aqueous solutions has been controlled by using several surfactants in premicellar conditions.[6−8] One of the successful methods for controlling porphyrin aggregation is the preparation of mixed Langmuir−Blodgett (LB) films containing a water-soluble porphyrin and a lipid anchor.[9−19]

In the present paper, the formation of the different aggregates of a water-soluble tetracationic porphyrin, TMPyP, anchored to an anionic phospholipid matrix, DMPA, and assembled in LB films has been investigated. The TMPyP/DMPA system with a molar ratio of 1:4 has been previously studied at the air−water interface where two different forms for the organization of the porphyrin depending on the surface pressure have been found. Thus, a monomeric form was found for low surface pressure ($\pi \leq 8$ mN/m) and a particular dimer at high surface pressure ($\pi > 35$ mN/m), both forms coexisting for intermediate surface pressures.[20] A particular structure has been proposed for the porphyrin dimer in which the parallel rings of the molecules are twisted by 45° with respect to each other (see Scheme 1).[20] The mixed 1:4 TMPyP/DMPA system, which corresponds to the stoichiometry of the molecular charges of the components, was transferred on hydrophilic glass at a surface pressure of 35 mN/m. The absorption spectrum obtained for

SCHEME 1: Structures of DMPA (vertical section) and TMPyP (in flat orientation) and the in-plane Configuration of Two Stacked Molecules of Porphyrin (dimer)

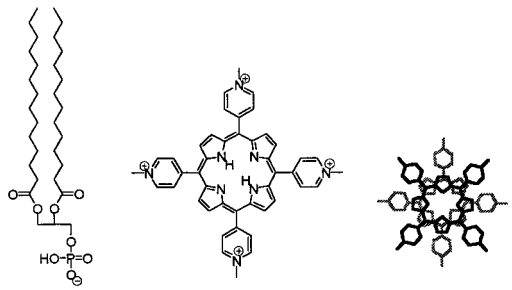

* Corresponding author. E-mail: qf1cadel@uco.es.
[†] Universidad de Vigo.
[‡] Universidad de Córdoba.
[§] Max-Planck-Institut für biophysikalische Chemie.

10.1021/jp0022306 CCC: $19.00
Published on Web 10/05/2000

the mixed monolayer demonstrated that only the monomeric form was present on the substrate. From the measurement of the transmission spectra without and with plane-polarized light (s and p) under various angles of incidence, the average orientation of the porphyrin molecules coplanar to the substrate was confirmed. Thus, the porphyrin molecules deposited on hydrophilic glass are sandwiched between the support and the highly ordered DMPA monolayer.

The use of different solid substrates such as hydrophilic glass and supports modified by transfer of monolayers of several lipids such as DMPA, eicosylamine, or arachidic acid in different sequences has enabled us to detect four different types of organization of the porphyrin molecules. These are the monomer ($TMPyP^{4+}$), the dimer, the diprotonated monomer ($TMPyPH_2^{6+}$), and the tetramer. The aim of this work is the identification and structural and spectroscopic characterization of these molecular aggregates of TMPyP formed in LB films.

Experimental Section

Material. Arachidic acid (AA) was purchased from E. Merck and recrystallized from ethanol. L-α-Dimyristoylphosphatidic acid, DMPA, was supplied by Sigma Chemical Co. and used as received. The 5,10,15,20-tetrakis(1-methyl-4-pyridyl)-21*H*,23*H*-porphine, TMPyP, was purchased from Aldrich Chemical Co. and used without further purification. Eicosylamine (EA) was prepared by W. Schulten at the MPI in Göttingen. Pure chloroform and a 3:1 (v/v) mixture of chloroform and methanol were used as spreading solvents. The pure solvents were obtained without further purification from Baker Chemicals. The water for the subphase was prepared with a Milli-Q filtration unit of Millipore Corp.

Fabrication of Monolayers. Monolayers were prepared by spreading solutions of AA, EA, or DMPA. Mixed monolayers were formed by cospreading 1:4 TMPyP/DMPA (TD) on a circular trough provided with a filter paper Wilhelmy plate.[21] The subphase was Milli-Q water at pH 5.6, and the temperature was kept constant at 21 °C. Monolayers were compressed by a movable Teflon barrier with a compression velocity of 0.05 nm^2 min^1 $molecule^{-1}$ and transferred onto glass plates at constant surface pressures of 20 and 40 mN/m for AA and EA, respectively, and 35 mN/m for DMPA and TD monolayers, respectively, by vertical dipping with a lifting speed of 5 mm min^{-1}.

The different systems were assembled by sequential monolayer transfer, i.e., immersion (↓) and withdrawal (↑). The transfer ratio, τ, for each monolayer will be shown in brackets.

The transferred systems were characterized by absorption spectroscopy. Details of the spectrometer have been described elsewhere.[22,23] The absorption here is expressed as the difference ΔT in the transmission of the reference section without the dye and the measuring section of the slide.

All the experiments were performed at least four times.

Results and Discussion

Figure 1 shows the transmission spectrum of a TD monolayer ($\tau = 0.97$) deposited on glass which was previously modified with the following sequence of monolayers: EA↑/AA↓/EA↑/AA↓ ($\tau = 0.97, 1, 1.03, 1$) (solid line). For comparison, the transmission spectrum of a TD monolayer transferred directly onto hydrophilic glass ($\tau = 1.03$) (dashed line)[20] and the reflection spectrum corresponding to a monolayer of TMPyP monomer at the air−water interface (dotted line)[20] are also shown.

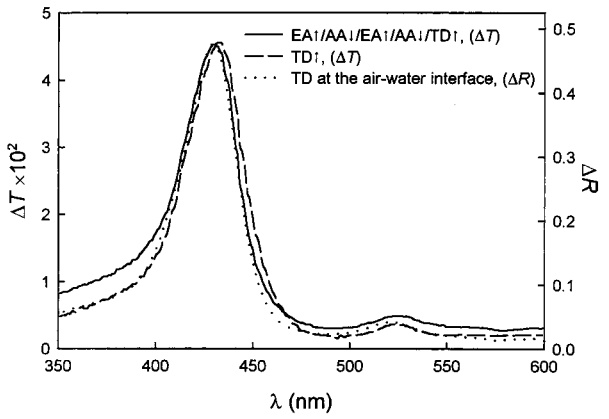

Figure 1. Absorption spectra the EA↑/AA↓/EA↑/AA↓/TD↑ assembly (solid line) and the TD↑ monolayer (dashed line) on hydrophilic glass. The dotted line corresponds to the reflection spectrum for the monomer porphyrin at the air−water interface ($\pi = 5$ mN/m).[20] Other considerations can be found in the text.

In the cases of low absorption values and no difference in the absorption spectrum of the solution and the transferred monolayer, the transmission, ΔT, is given in a reasonable approximation by[23]

$$\Delta T = 2.303 f_{\text{orient}} \epsilon \Gamma [1 + \sqrt{R_g}] 10^3 \qquad (1)$$

where f_{orient} is a numerical factor that takes into account the different orientation of the porphyrin in the monolayer as compared to the random orientation in solution, ϵ is the extinction coefficient given as L mol^{-1} cm^{-1}, Γ is the surface concentration measured by mol cm^{-2}, $R_g = 0.042$ is the reflectivity of glass at the air−glass interface, and 10^3 (conversion of L to cm^3) is a numerical factor. The value of $\Delta T = 0.0433$ at the maximum has been obtained under the following assumptions: the extinction coefficient for the porphyrin at the air−water interface is the same as in that the spreading solution, a surface concentration of TMPyP is equivalent to one monolayer, i.e., 5.2×10^{-11} mol/cm^2, and an average planar orientation for the ring of the porphyrin molecules with respect to the support surface must be $f_{\text{orient}} = 1.5$.[20] This calculated value coincides with the experimental value $\Delta T = 0.0455$.

The strong resemblance of shapes and heights of the spectra shown in Figure 1 unambiguously shows that the TMPyP is transferred only as monomer in those types of monolayers.[20] The absorption spectrum of the TMPyP monomer shows the typical Soret band and four weak Q bands. The Soret band for the TMPyP monomer at the air−water interface has the maximum at 430 nm (Figure 1, dotted line), like in the spreading solution. The maximum of the Soret band appears at 433 nm when the transfer is performed on hydrophilic glass and the porphyrin is directly bound to the substrate (Figure 1, dashed line).[20] If the glass and the porphyrin are separated by spacer layers such as the monolayer sequence EA↑/AA↓/EA↑/AA↓, the maximum is again observed at 430 nm (Figure 1, solid line). The small difference of 3 nm found between the last two spectra may be attributed to the different environment of the porphyrin.

To determine the average orientation of the porphyrin molecules in the monolayer of EA↑/AA↓/EA↑/AA↓/TD↑ (Figure 1, solid line), the absorption spectra were measured with and without polarized light, s and p, under angles of incidence of 30° and 45°, respectively. The results presented as ratios of the absorption values ΔT, i.e., $\Delta T_s/\Delta T_n$ and $\Delta T_s/\Delta T_p$, are listed in Table 1. Also, the theoretical values for a planar orientation of the porphyrin ring given by Orrit et al.[24] are shown in Table 1.

TABLE 1: Values of ΔT Ratios at Several Angles of Incidence Measured for Different LB Films[a]

	30°		45°	
LB films	$\Delta T_s/\Delta T_n$	$\Delta T_s/\Delta T_p$	$\Delta T_s/\Delta T_n$	$\Delta T_s/\Delta T_p$
EA↑/AA↓/EA↑/AA↓/TD↑ ($\lambda = 430$ nm)	1.10	1.20	1.25	1.49
TD↑/(DMPA↓/TD↑)$_n$ − TD↑ ($\lambda = 416$ nm)	1.05	1.14	1.17	1.36
TD↑/(TD↓/TD↑)$_n$ − TD↑ ($\lambda = 400$ nm)	1.08	1.19	1.26	1.43
theoretical values for a plane orientation[24]	1.10	1.19	1.24	1.50

[a] The data are average values from the measured spectra. Theoretical values for a plane orientation of the porphyrin ring parallel to the monolayer plane are also included.

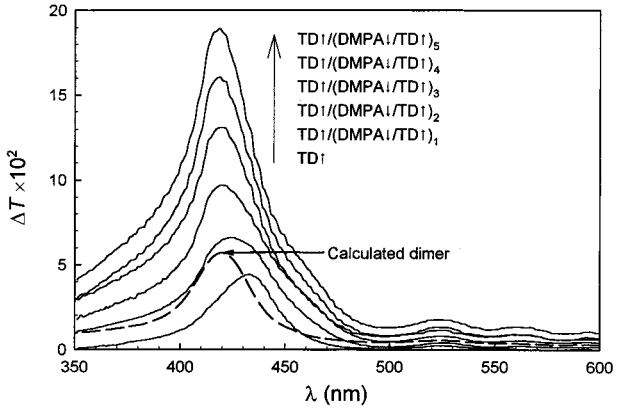

Figure 2. Spectra of consecutive TD↑(DMPA↓/TD↑)$_n$ films for $n = 0-5$ (solid lines). The dashed line corresponds to the evaluated spectrum of dimer.[20] Other considerations are in the text.

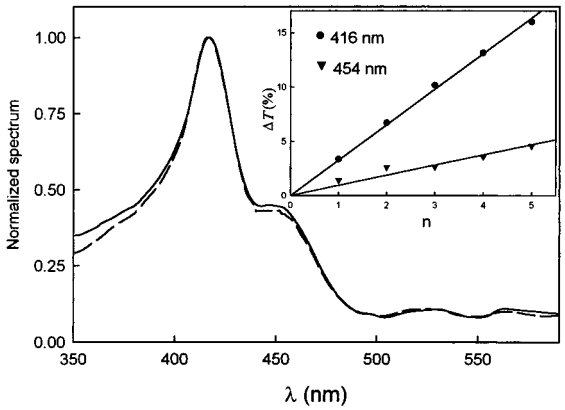

Figure 3. Normalized spectra of [TD↑/(DMPA↓/TD↑)$_1$ − TD↑] (solid line) and [TD↑/(DMPA↓/TD↑)$_2$ − TD↑] (dashed line). The inset plots the transmission values at 416 nm (circles) and 454 nm (triangles) for the [TD↑/(DMPA↓/TD↑)$_n$ − TD↑] spectra vs n.

As can be seen, there is a very good coincidence between the experimental and calculated data for an orientation of the porphyrin ring parallel to the monolayer plane.

Porphyrin dimers are formed at the air−water interface in monolayers of 1:4 TMPyP/DMPA[20] and may be transferred to solid substrates. Figure 2 shows the absorption spectrum of the LB film of TD↑/DMPA↓/TD↑ ($\tau = 1.03, 0.71, 1$), the fifth full line from the top. This spectrum is quite different from those shown in Figure 1. The broad shape of the Soret band means that such a spectrum has contributions from both the monomer and dimer forms. The dimer reflection spectrum of TMPyP has been evaluated at the air−water interface by analyzing the reflection spectra of a TMPyP/DMPA monolayer measured at different surface pressures.[20] This reflection spectrum may be transformed to an absorption spectrum by the ratio $\Delta T/\Delta R = (1 + \sqrt{R_g})/\sqrt{R_w}$, where R_g and R_w are the reflectivity of the glass and the water, respectively,[24] assuming the same orientation in the transferred layer as on water; the result is shown as the dashed line of Figure 2.

The Soret band for the dimer form of TMPyP in this absorption spectrum has the maximum at 420 nm.[20]

To evaluate more carefully the contribution of dimers, we prepared LB films assembled by sequential monolayer transfer TD↑/(DMPA↓/TD↑)$_n$ ($0 \le n \le 5$). The measured absorption spectra are shown in Figure 2. In these films, the transfer process was as follows: the mixed monolayers containing TMPyP, i.e., TD, were always transferred during the withdrawal of substrate from the aqueous subphase ($\tau \approx 1$), while the phospholipid layers, i.e., DMPA, were deposited by immersion ($\tau \approx 0.7$).

The absorption ΔT shown in Figure 2 increases with increasing the number of layers transferred onto the hydrophilic glass plates. A blue-shift of the Soret band with the number of layers transferred is observed in the series of spectra. Thus, the λ_{max} value of the Soret band is shifted from 433 nm for the TD↑ sample to 416 nm for the TD↑/(DMPA↓/TD↑)$_5$ system. This phenomenon is related to the predominant presence of the porphyrin dimer in such LB films when the number of deposited layers increases. Furthermore, those spectra show, as an additional feature, the appearance of a shoulder around 460 nm.

To resolve both the contribution and the kind of different aggregates of TMPyP in the LB films whose spectra are shown in Figure 2, we subtracted the spectrum of the TD↑ monolayer corresponding to a monolayer of monomeric porphyrin from the rest of spectra.

A sample of the results of this evaluation, including normalization to the same maximum value, is shown in Figure 3, where the solid line represents the normalized spectrum resulting from the difference of [TD↑/DMPA↓/TD↑] − [TD↑] and the dashed line is the corresponding spectrum obtained as difference of [TD↑/(DMPA↓/TD↑)$_2$] − [TD↑].

A very good agreement between the difference spectra for $n = 1$ and $n = 2$ is obtained, and this phenomenon is observed for any value of n (data not shown here due to that coincidence). The maximum of the Soret band for all difference spectra remains constant at 416 nm. A good agreement is obtained by comparison of those spectra with that corresponding to the dimer (Figure 2, dashed line), except for the shoulder at 454 nm. Thus, the band at 416 nm can be ascribed to the porphyrin dimer. The new absorption maximum at 454 nm will be discussed below. The behavior shown in Figure 3 allows us to conclude that the monomer form of TMPyP is only transferred in the first layer of the TD↑/(DMPA↓/TD↑)$_n$ LB films, whereas the porphyrin is organized as a dimer in the subsequent monolayers assembled; however, there is a new species responsible of the absorption band at 454 nm.

Various reasons may be responsible for the shift of the Soret band to longer waves. We rule out a metalation of the macrocycle by heavy metal ions causing such a shift. Another possible reason could be torsion of the methylpyridyl groups to an orientation more parallel to the macrocycle, as recently observed for TMPyP adsorbed to Laponite.[25] This phenomenon has been related to nonelectrostatic interactions. In the systems

investigated here, i.e., mixed monolayers of TMPyP/DMPA, the porphyrin is attached to DMPA via electrostatic interactions. Therefore, such an explanation does not apply to our case. Further, association of the porphyrin to J aggregates may cause a shift of the Soret band to longer waves. Such a phenomenon has been observed with neutral picket-fence porphyrins (4,0-tetrakis(amidophenyl)porphyrins) in surfactant solutions[6] and with the diprotonated tetrakis-(4-sulfonatophenyl)porphine (H_4TPPS^{2-}) in aqueous acidic surfactant solutions.[8] In the latter case, the Soret band maximum is at 492 nm, and the region of the Q bands is drastically changed with the appearance of a new band at 706 nm. In the case of the monolayer assemblies, the Q band region does not show any modification similar to those found in the aqueous surfactant solutions. To our knowlegde, no formation of J aggregates has been reported in the literature for TMPyP. The formation of J aggregates as a reason for the appearance of the 454 nm band, therefore, is also ruled out.

The assignment of the 454 nm band to the diprotonated form of TMPyP is the most reasonable explanation. Several observations support this interpretation. In monolayers at the air−water interface of an amphiphilic analogue of TMPyP with the maximum of the Soret band at 430 nm, a new band at 450 nm was found by titration that has been attributed to the diprotonated porphyrin.[26] The Soret band of the TMPyP monomer in a micellar surfactant solution shifts from 426 to 444 nm upon formation of the diprotonated form.[8] In aqueous solution at neutral pH, the maximum of the Soret band is at 422 nm, whereas in a 1 M HCl solution, it is at 448 nm (see, e.g., ref 25). The only difficulty in attributing the band at 454 nm to the diprotonated form of TMPyP seems to account for the apparent p*K* of the diacid formed in the monolayer assemblies, since the monolayers have been transferred from an aqueous subphase of pH 5.6. At this point, we have to consider the particular situation in monolayers and monolayer assemblies. Both the interfacial pH and the intrinsic p*K* of a probe depend on the composition of the headgroup region as well as on the remote environment. A modification of the composition of the interface at a distance of 5.4 nm may cause a shift of the apparent p*K* of a pH probe at the assembly−water interface by approximately 5 p*K* units.[27]

Another study reports a shift of the apparent p*K* of a pH probe at the assembly−water interface upon the modification of the hydrophobic interface at a distance of 2.7 nm of ∼3 p*K* units.[28]

Therefore, it is conceivable that a molecule of TMPyP may be protonated upon transfer when facing undissociated DMPA molecules. Indeed, the TD monolayers transferred at a surface pressure of 35 mN/m contain a small fraction of monomers of approximately 0.12.[20]

These monomers then may interact with the headgroups of the DMPA molecules in the preceding monolayer, forming the diprotonated TMPyP and DMPA anions as shown in Scheme 2 (only the DMPA molecules directly interacting with TMPyP are represented here).

The spectra with and without polarized light under different angles of incidence were measured to determine the average orientation of the dimer in TD↑/(DMPA↓/TD↑)$_n$ films after subtracting the contribution of the monomers, i.e., [TD↑/(DMPA↓/TD↑)$_n$ − TD↑]. The ratios $\Delta T_s/\Delta T_p$ and $\Delta T_s/\Delta T_n$ were obtained by measuring the transmission spectra with polarized light of the TD↑/(DMPA↓/TD↑)$_n$ and TD↑ films. The values determined at 416 nm are shown in Table 1. The values are slightly smaller than the theoretical ratios[24] for a plane orientation of the porphyrin. With these values and by the treatment of Orrit et al.,[24] it is possible to estimate an inclination of ∼10° for the plane of the porphyrin dimer with respect to the substrate surface. This phenomenon may be attributed to defects of the preceding layers in the assembly.

SCHEME 2: Model of Organization of $TMPyPH_2^{6+}$ from Electrostatic Interactions with DMPA Molecules[a]

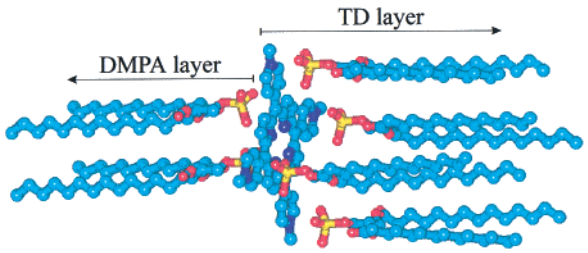

[a] The Four top DMPA molecules (from the TD↑ layer) interact with the four pyridyl groups, and the two bottom DMPA molecules (from the DMPA↑ layer) interact with the two positive charges of the central ring of the porphyrin. Only the DMPA molecules directly interacting with TMPyP are represented.

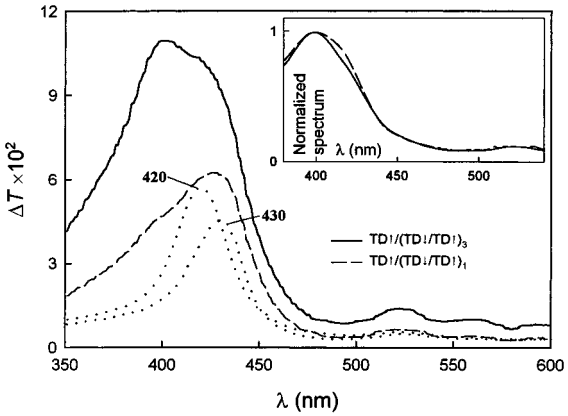

Figure 4. Absorption spectra of TD↑/(TD↓/TD↑)$_3$ film (solid line) and TD↑/(TD↓/TD↑)$_1$ film (dashed line). The dotted lines correspond to the dimer-evaluated spectrum from the air−water interface (420 nm) and the EA↑/AA↓/EA↑/AA↓/TD↑ monolayer (430 nm). The inset shows the normalized spectra of [TD↑/(TD↓/TD↑)$_n$ − TD↑] for $n = 3$ (solid line) and $n = 1$ (dashed line).

The inset of Figure 3 shows the values of ΔT for the two wavelengths λ_{max} of the species discussed before, i.e., 416 and 454 nm, corresponding to spectra of [TD↑/(DMPA↓/TD↑)$_n$ − TD↑] versus n. A linear relationship is found for both species. The linear relationship between the number of layers and the absorption of the two bands, at 416 and 454 nm, indicates that the fractions of the porphyrin transferred in each monolayer as either a dimer or a diprotonated monomer, respectively, are almost constant.

Furthermore, a new type of porphyrin aggregate is observed when monolayers with the sequence of TD↑/(TD↓/TD↑)$_n$ were transferred on hydrophilic glass plates. Figure 4 shows the spectra of those LB films corresponding to the deposition of films with $n = 3$ (solid line) and $n = 1$ (dashed line). The transfer ratio is close to unity when the support is withdrawn from the aqueous subphase through the monolayer formed at the air−water interface and 0.6 during the immersion process.

Also, this figure shows as reference the spectra (dotted lines) obtained both for the monomer monolayer, EA↑/AA↓/EA↑/AA↓/TD↑ (from Figure 1), and for the dimer monolayer (from Figure 2), with $\lambda_{max} = 430$ and 420 nm, respectively.

The spectra of the TD↑/(TD↓/TD↑)$_n$ multilayers show not only an increase of ΔT with increasing n but also a new absorption

band at 400 nm. We propose that this band is related to the formation of porphyrin tetramers, as discussed later.

To eliminate the contribution of the monomer of the first layer, we calculated the difference spectra [TD↑/(TD↓/TD↑)$_n$] − [TD↑]. The results thus obtained and after normalizing to the same maximum value are not completely coincident (inset in Figure 4). The difference is mainly found in the region close to 420 nm. This phenomenon can be related to the fact that the porphyrin in this type of film is partially transferred as a dimer whose fraction seems to be different in each subsequent layer. Thus, the dimer fraction is higher for the [TD↑/(TD↓/TD↑)$_1$] − [TD↑] system (dashed line) than for the [TD↑/(TD↓/TD↑)$_3$] − [TD↑] system (solid line). Furthermore, the band at 454 nm is absent in these spectra. This supports the assignment of that band to the diprotonated porphyrin (see above), since the small fraction of the porphyrin monomers, upon transfer by withdrawal (↑), do not face the DMPA molecules.

Furthermore, the values of absorption ΔT with polarized light (s and p) under different angles of incidence were determined. The results for the difference spectra [TD↑/(TD↓/TD↑)$_n$] − [TD↑] at 400 nm are shown in Table 1 and confirm an approximately flat orientation of the species having this absorption maximum with respect to the surface.

To determine the aggregation number, we calculated the spectral shift for the aggregate with respect to the monomer using the extended-dipole approximation.[29] According to this model, the excitation energy of the dye dimer can be given by the relation

$$\Delta E_{\text{dim}} = \Delta E_{\text{mon}} + V + 2J_{1,2} \qquad (2)$$

where ΔE_{mon} is the excitation energy of the dye monomer, V is a dispersion energy term that reflects the change in environment, and $J_{1,2}$ is the interaction energy between molecules.

The maximum of the Soret band for the porphyrin dimer at the air−water interface was shifted 10 nm to shorter waves with respect to the monomer. Thus, $\Delta E_{\text{dim}} - \Delta E_{\text{mon}} = 0.07$ eV [λ_{max}(mon) = 430 nm and λ_{max}(dim) = 420 nm].[20] We consider a porphyrin dimer with a 45° twist of parallel rings (Scheme 1). A model of the porphyrin dimer as shown in Scheme 1 appears to be very reasonable, since steric hindrance of the methylpyridyl rings is avoided by twisting and close contact of the macrocycles is enabled. Crystal structures with different organization are not comparable because the porphyrin molecules experience a totally different environment in the investigated systems and are organized under external pressure. Face-to-face stacking of porphyrin rings occurs in monolayers as shown, e.g., in the case of μ-oxo dimer formation of iron porphyrins in organized monolayer assemblies.[30]

A blue-shift of 9 nm was calculated with the extended dipole approximation using the following parameters: a dipole length of $l = 0.38$ nm, a charge of $\epsilon = 0.22$e, a dielectric constant of $D = 2.5$, a thickness of the porphyrin of 0.35 nm, and $V = 0$.[20]

However, the blue-shift of the Soret band due to the dimer formation on glass is larger than that observed at the air−water interface. In fact, λ_{max}(mon) = 430 nm while λ_{max}(dim) = 416 nm, and therefore, $\Delta E_{\text{dim}} - \Delta E_{\text{mon}} = 0.1$ eV = −14 nm. This increase of the $\Delta E_{\text{dim}} - \Delta E_{\text{mon}}$ value can be attributed to the V of eq 2, $V \approx 0.03$ eV. On glass, the dimer aggregate is only assembled when the TMPyP molecules are sandwiched between two chains of DMPA, which excludes the presence of monomers.

Equation 2 has to be modified for aggregates with aggregation numbers >2 (see Appendix).

SCHEME 3: Modeling of the Packed Tetramer for TMPyP, Together with the DMPA Molecules in (TD↓/TD↑)$_n$ LB Films (vertical section)[a]

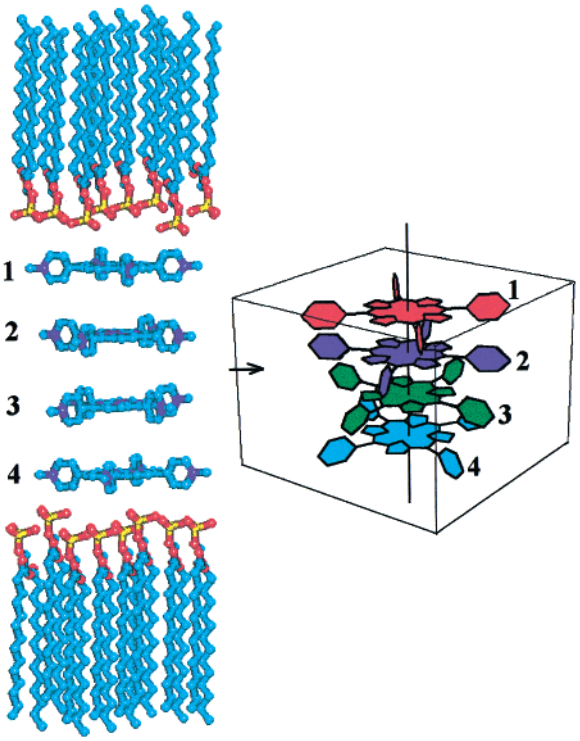

[a] A perspective view of the tetramer containing the four molecules of porphyrin is drawn. The number indicates the assigned position of the molecules in the tetramer aggregate.

In this work, we propose the formation of a packed tetramer of porphyrin molecules associated face-to-face (see Scheme 3). Furthermore, it is assumed that the distance between planes of two consecutive porphyrins and of the dimer is 0.35 nm.[20] However, to minimize the possible steric hindrance between the positive methylpyridyl groups of adjacent molecules, which are oriented with their plane nearly perpendicular to that of the central ring of the porphyrin, we formulated an additional consideration: the central planes of the porphyrin molecules compose a sort of helix where the planes between consecutive porphyrin molecules are twisted by 22.5°. According to this-organization, the excitation energy of the dye tetramer (see Appendix) can be given by the relation

$$\Delta E_{\text{tetra}} = \Delta E_{\text{mon}} + V + 2J_{1,2} + J_{1,3} + J_{1,4} \qquad (3)$$

where the positions of the different molecules are indicated by subindices 1, 2, 3, and 4 (see Scheme 3) and $J_{1,3}$ and $J_{1,4}$ are the interaction energies between the non-nearest neighbor molecules.

By this procedure and with $V = 0.03$ eV, we obtain a good agreement between the experimental and theoretical data. In fact, using this value of V, we calculated the excitation energy for the tetramer aggregate to be $\Delta E_{\text{tetra}} - \Delta E_{\text{mon}} = 0.22$ eV, resulting in a shift of $\Delta\lambda_{\text{tetra}} = \lambda_{\text{tetra}} - \lambda_{\text{mon}} = -26$ nm, which is very close to the experimental blue-shift of −30 nm measured in Figure 4 [λ_{max}(mon) = 430 nm and λ_{max}(tetra) = 400 nm]. For alternative models with different organization of the porphyrin molecules, the calculated shifts are slightly different (see Appendix). In this discussion, we have assumed the organization in Scheme 3 since it has the maximum $\Delta\lambda_{\text{tetra}}$ shift.

SCHEME 4: Organization of Stacked Dipoles with the Geometrical Center Placed on the *z* Axis and Spaced at Distance *r*[a]

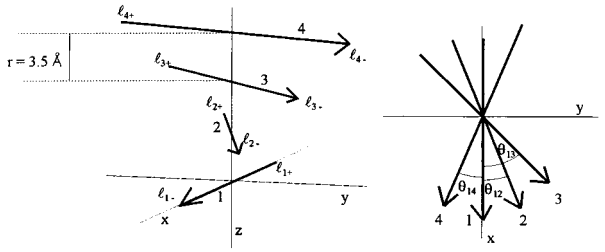

[a] θ_{12}, θ_{13}, and θ_{14} are the angles between the dipoles of the porphyrin molecules.

Conclusion

In this paper, it has been demonstrated that the Langmuir−Blodgett technique using mixed films containing a water-soluble porphyrin and a phospholipid anchor is successful for the control of the orientation and aggregation of the porphyrin. The transfer of organized monolayers on solid substrates with hydrophilic surfaces has enabled us to prepare various aggregates of a cationic water-soluble porphyrin. Thus, the TMPyP molecules in the mixed monolayer with DMPA in a molar ratio of 1:4 have been assembled as monomer ($TMPyP^{4+}$), dimer, diprotonated monomer ($TMPyPH_2^{6+}$), and tetramer aggregates, depending on the method employed.

The porphyrin is organized as a monomer ($TMPyP^{4+}$) when the mixed monolayer is directly transferred onto a hydrophilic glass plate. Likewise, this species of porphyrin is detected when the glass surface is modified with the monolayer sequence EA↑/AA↓/EA↑/AA↓. However, the dimer is obtained by the transfer of the 1:4 TMPyP/DMPA on top of a DMPA monolayer $(DMPA↓/TD↑)_n$. Here, the porphyrin molecules are sandwiched between the polar groups of two layers of the phospholipid. Furthermore, in these multilayers, a new band at 454 nm was observed. We propose that this new band is due to the protonation of the central ring of the porphyrin molecule to form $TMPyPH_2^{6+}$ by the interaction of a small fraction of $TMPyP^{4+}$ monomers with the acidic groups of DMPA in the preceding monolayer. Thus, the new organization has six molecules of DMPA compensating six positive charges of one molecule of porphyrin, four residing on the pyridyl goups and two on the central ring (see Scheme 2).

Finally, the transfer on hydrophilic glass plates of TD monolayers of the Y type assembled a packed tetramer of TMPyP. By applying the extended dipole approximation to the spectra measured, we proposed a model where the central planes of the two consecutive porphyrins are twisted by 22.5°, forming a helix (see Scheme 3). However, together with the tetramer, the dimer form is also transferred, and the dimer fraction decreases with the increasing number of transferred monolayers.

Appendix

In the extended dipole approximation, the molecules are replaced by dipoles of fixed length (l), charge (ϵ), and orientation.[29] In this work, we have assumed an organization of stacked dipoles as shown in Scheme 4, where the geometrical centers of the dipoles, spaced at distance r, are placed on the z axis. Thus, only the rotation of the dipole around such a center is allowed.

The coordinates of the positive and negative ends of each dipole, i, are designated as l_{i^+} and l_{i^-}, and $l = |l_{i^+} - l_{i^-}|$. The distance between ends with the same sign of two different dipoles, i and j, is given by the relation

$$a_{i,j} = |l_{i^+} - l_{j^+}| = |l_{i^-} - l_{j^-}| = \sqrt{\frac{l^2}{2}[1 - \cos(\theta_{i,j})] + [(i-j)r]^2} \quad \text{(A1)}$$

Likewise, the distance between ends with different sign is

$$b_{i,j} = |l_{i^+} - l_{j^-}| = |l_{i^-} - l_{j^+}| = \sqrt{\frac{l^2}{2}[1 + \cos(\theta_{i,j})] + [(i-j)r]^2} \quad \text{(A2)}$$

where $\theta_{i,j}$ is the angle between dipoles (see Scheme 4). The interaction energy between two any dipoles will be[29]

$$J_{i,j} = \frac{\epsilon^2}{D}\left[\frac{2}{a_{i,j}} - \frac{2}{b_{i,j}}\right] \quad \text{(A3)}$$

where D is the dielectric constant. Finally, the average interaction energy of a stacked aggregate with N dipoles can be related by

$$\Delta E_{aggr} = \Delta E_{mon} + V + 2\sum_{i \neq j}\frac{J_{i,j}}{N} \quad \text{(A4)}$$

Assuming a stacked structure where the angle between two consecutive dipoles is constant, the relation $J_{1,2} = J_{2,3} = J_{3,4} = ...$, $J_{1,3} = J_{2,4} = ...$ is accomplished. Therefore, eq A4 is changed to

$$\Delta E_{aggr} = \Delta E_{mon} + V + 2J_{1,2} \times \frac{2(N-1)}{N} + 2J_{1,3}\frac{2(N-2)}{N} + 2J_{1,4}\frac{2(N-3)}{N} + ... \quad \text{(A5)}$$

In the model in Scheme 4 (tetramer, $N = 4$), the dipole composes a sort of helix where consecutive porphyrin molecules are twisted by 22.5° and the eq A5 is reduced to

$$\Delta E_{tetra} = \Delta E_{mon} + V + 3J_{1,2} + 2J_{1,3} + J_{1,4} \quad \text{(A6)}$$

The shift of the absorption maximum, $\Delta\lambda_{tetra} = \lambda_{tetra} - \lambda_{mon}$, can be calculated by

$$\Delta\lambda_{tetra} = \lambda_{tetra} - \lambda_{mono} = -\frac{\lambda_{mono}}{1 + \frac{hc}{(\Delta E_{tetra} - \Delta E_{mono})\lambda_{mono}}} \quad \text{(A7)}$$

The excitation energy for the tetramer is $\Delta E_{tetra} - \Delta E_{mon} = 0.22$ eV, resulting in a shift of $\Delta\lambda_{tetra} = \lambda_{tetra} - \lambda_{mon} = -26$ nm, assuming the organization in Scheme 4 and assuming $V = 0.03$ eV, $I = 0.38$ nm, $\epsilon = 0.22$e, and D = 2.5, parameters coincident with those used for the theoretical treatment of the dimer.[20]

Two alternative organizations with respect to that shown in Scheme 4 have been considered. For example, the positions of dipoles 3 and 4 have been alternated, with $\theta_{2,3} = 45°$; thus, $J_{2,3} = J_{1,2} = J_{3,4}$, and eq A4 becomes

$$\Delta E_{tetra} = \Delta E_{mon} + V + 2J_{1,2} + J_{2,3} + 2J_{1,3} + J_{1,4} \quad \text{(A8)}$$

With $V = 0.03$ eV, a shift of $\Delta\lambda_{tetra} = \lambda_{tetra} - \lambda_{mon} = -25$ nm is obtained.

Finally, the positions of dipoles 2 and 3 have been alternated with respect to those shown in Scheme 4. Thus, $\theta_{1,2} = \theta_{3,4} =$

45° and $\theta_{2,3} = 22.5°$, and the mathematical expression corresponding to ΔE_{tetra} is identical to eq A8, although the values of $J_{i,j}$ are different. In this organization and with $V = 0.03$ eV, the resulting shift is $\Delta\lambda_{tetra} = \lambda_{tetra} - \lambda_{mon} = -24$ nm.

References and Notes

(1) Miyama, S., Nalwa, H. S., Eds. In *Organic Electroluminescent Materials and Devices*; Gordon and Breach: Amsterdam, 1997.

(2) Tang, C. W.; van Slyke, S. A. *Appl. Phys. Lett.* **1987**, *51*, 913.

(3) Yang, Y. *MRS Bull.* **1997**, *22*, 31.

(4) Stapff, I. H.; Stümpflen, V.; Wendorff, J. H.; Spohn, D. B.; Möbius, D. *Liq. Cryst.* **1997**, *23*, 613.

(5) Gandini, S. C. M.; Borissevitch, I. E.; Perusi, J. R.; Imasato, H.; Tabak, M. *J. Lumin.* **1998**, *78*, 53.

(6) Barber, D. C.; Freitag-Beeston, R. A.; Whitten, D. G. *J. Phys. Chem.* **1991**, *95*, 4074.

(7) Maiti, N. C.; Mazumdar, S.; Periasamy, N. *Curr. Sci.* **1996**, *70*, 997.

(8) Maiti, N. C.; Mazumdar, S.; Periasamy, N. *J. Phys. Chem. B* **1998**, *102*, 1528.

(9) Schick, G. A.; Schreiman, I. C.; Wagner, R. W.; Lindsey, J. S.; Bocian, D. F. *J. Am. Chem. Soc.* **1989**, *111*, 1344.

(10) Möbius, D.; Grüniger, H. R. *Bioelectrochem. Bioenerg.* **1984**, *12*, 375.

(11) Möbius, D. *Z. Phys. Chem. Neue Folge* **1987**, *154*, 121.

(12) Gust, D.; Moore, T. A.; Moore, A. L.; Luttrull, D. K.; DeGraziano, J. M.; Boldt, N. J.; Van der Auweraer, M.; De Schryver, F. C. *Langmuir* **1991**, *7*, 1483.

(13) Cordroch, W.; Möbius, D. *Thin Solid Films* **1992**, *210/211*, 135.

(14) Azumi, R.: Matsumoto, M.; Kawabata, Y.; Kuroda, S.; Sugi, M. *J. Am. Chem. Soc.* **1992**, *114*, 10662.

(15) Yoneyama, M.; Fujii, A.; Maeda, S.; Murayama, T. *J. Phys. Chem.* **1992**, *96*, 9882.

(16) Azumi, R.; Matsumoto, M.; Kawabata, Y.; Kuroda, S.; Sugi, M.; King, L. G.; Crossley, M. J. *J. Phys. Chem.* **1993**, *97*, 12862.

(17) Martin, M. T.; Möbius, D. *Thin Solid Films* **1996**, *284/285*, 663.

(18) Zhang, Z.; Nakashima, K.; Verma, A. L.; Yoneyama, M.; Iriyama, K.; Ozaki, Y. *Langmuir* **1998**, *14*, 1177 and references therein.

(19) De Cruz, F.; Armand, F.; Albouy, P.-A.; Nierlich, M.; Ruaudel-Teixier, A. *Langmuir* **1999**, *15*, 3653.

(20) Martin, M. T.; Prieto, I.; Camacho, L.; Möbius, D. *Langmuir* **1996**, *12*, 6554.

(21) Fromherz, P. *Rev. Sci. Instrum.* **1975**, *46*, 1380.

(22) Kuhn, H.; Möbius, D.; Bücher, H. In *Spectroscopy of Monolayer Assemblies*; Weissberger, A., Rossiter, B. W., Eds.; Wiley: New York, 1972; Vol. I, Part IIIB, p 656.

(23) Griiniger, H.; Möbius, D.; Meyer, H. *J. Chem. Phys.* **1983**, *79*, 3701.

(24) Orrit, M.; Möbius, D.; Lehmann, U.; Meyer, H. *J. Chem. Phys.* **1986**, *85*, 4966.

(25) Chernia, Z.; Gill, D. *Langmuir* **1999**, *15*, 1625.

(26) Loschek, R.; Möbius, D. *J. Chim. Phys.* **1988**, *85*, 1041.

(27) Petrov, J. G.; Möbius, D. *Langmuir* **1991**, *7*, 1495.

(28) Möbius, D.; Ahuja, R. C.; Caminati, G.; Chi, L. F.; Cordroch, W.; Li, Z.; Matsumoto, M. In *Dynamics and Mechanisms of Photoinduced Transfer and Related Phenomena*; Mataga, N., Okada, T., Masuhara, H., Eds.; Elsevier Science: New York, 1992; p 377.

(29) Czikkely, V.; Försterling, H. D.; Kuhn, H. *Chem. Phys. Lett.* **1970**, *6*, 207.

(30) Hopf, F. R.; Möbius, D.; Whitten, D. G. *J. Am. Chem. Soc.* **1976**, *98*, 1584.